

On the use of NaI scintillation for high stability nuclear decay rate measurements

Scott D. Bergeson & Michael J. Ware

BYU Physics and Astronomy, Provo, UT 84602

Jeremy Hawk

Utah Valley Regional Medical Center, Provo, UT 84602

Abstract

We demonstrate the linearity and stability of a gamma-ray scintillation detector comprised of a NaI(Tl) crystal and a scientific-grade CMOS camera. After calibration, this detector exhibits excellent linearity more than three decades of activity levels. Because the detector is not counting pulses, no dead-time correction is required. When high activity sources are brought into close proximity to the NaI crystal, several minutes are required for the scintillation to achieve a steady state. On longer time scales, we measure drifts of a few percent over several days. These instabilities have important implications for precision determinations of nuclear decay rate stability.

Keywords: Gamma-ray detector, CMOS image sensors, NaI(Tl) scintillator

1. Introduction

High quality nuclear decay rate measurements require detectors with good sensitivity, stability, and linearity. Depending on the measurement objectives and experimental environment, the detector may also need to provide energy resolution, timing information, and absolute activity levels. Under ideal conditions, activity measurements are limited by Poisson statistics. Generally speaking, the statistical limits allow improved accuracy for higher activity samples or for longer measurement times. However, it sometimes happens that high activity and long measurement times compromise the sensitivity, stability, or linearity of the detector.

Improving the stability of nuclear activity measurements is particularly important for determining variations in nuclear decay rates [4, 10]. It has been suggested that some beta-decay processes are linked to solar activity. The state-of-the-art limits on measurements of this solar-dependence is 0.01% or perhaps slightly lower [13, 2], but the accuracy of these limits is determined completely by detector instability [14]. Many decay processes result in the emission of gamma radiation. Thus, improving the stability of gamma-radiation detectors will help in determining the amplitude of a seasonally dependence in nuclear decay rate.

Most gamma-ray measurements can be divided into two processes. The first converts the gamma radiation into an electronic or photonic signal—ionization in a gas chamber, electron-hole production in a solid, scintillation in a solid, gas or liquid, and so forth. The second measurement process detects and records this electronic or photonic signal, sometimes with additional signal conditioning. High reliability measurements require both of these processes to operate flawlessly.

These processes sometimes display systematic dependencies on the measurement environment or configuration [13, 16]. For example, the measured count rate from a Geiger-Müller tube depends exponentially on the operating voltage. It also depends on the ambient pressure. As another example, scintillation detectors using photomultiplier tubes are unable to reliably measure high activity samples because of excessive dead-time correction. Limitations like these determine the kinds of measurements that these detectors can make.

In this paper we demonstrate some characteristics and limitations of a gamma radiation detector consisting of a NaI(Tl) crystal and a scientific grade camera. We show that the camera has good stability and acceptable linearity. We also show non-linearities and instabilities in NaI scintillation at high activity levels. The regime in which we work uses higher activity samples than can be used in traditional scintillation measurements due to dead-time issues. This is made possible by the single-photon sensitivity and multi-channel nature of the camera.

2. Experimental details

The equipment consists of a scientific camera, a NaI(Tl) scintillator crystal, and the radioactive sample (see Fig. 1). Similar scintillator-camera detector configurations have been used for gamma- and x-ray detection in previous studies [3, 6, 9, 15, 8, 7, 11]. However, the present work differs in that the entire camera is used as a “single-channel” detector, without either energy resolution, imaging information, or photo-electron amplification. The scientific camera could be used to detect gamma radiation without the scintillation crystal [12]. The thin silicon camera architecture could be used as a kind of proportional detector. However, our detector in this configuration is

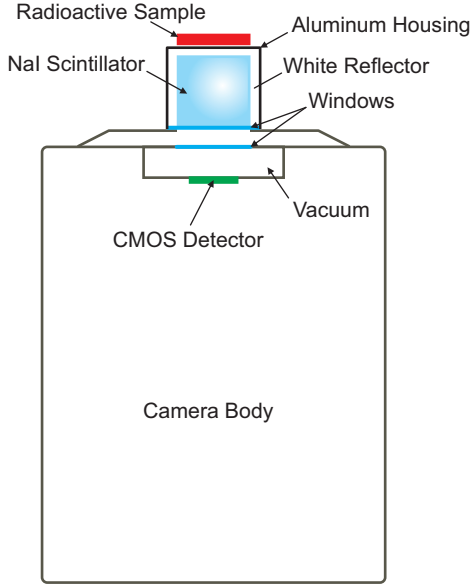


Figure 1: Schematic of a typical experimental setup. A radioactive sample is placed very near the aluminum housing of a NaI scintillation crystal. The crystal is mounted in a light-tight manner to the top of the camera, directly above the CMOS detector.

not as efficient as other materials used previously [5].

A simplified schematic of our setup is shown in Fig. 1. We use the Andor Neo 5.5 CMOS camera. The camera’s CMOS detector is cooled to -30°C , and the dark signal in the camera is less than 0.1 photo-electrons/pixel/second. A cylindrical NaI crystal, 25.4 mm in diameter and 25.4 mm in length, is attached directly to the lens mount of the camera via a light-tight housing (no focusing optics are used). The crystal is encased in a sealed aluminum housing with a glass window on one end of the cylinder allowing the scintillation photons to be detected by the camera. The NaI crystal housing is temperature controlled to approximately $\pm 0.002^{\circ}\text{C}$. Although the NaI crystal scintillation efficiency is not overly sensitive to temperature, the CMOS detector background level appears to change when the crystal temperature changes.

In this setup, gamma radiation from the sample causes scintillation in the crystal. The scintillation light is detected by the CMOS chip below, and the measured signal is the pixel grayscale in each camera image. The data reported here use the camera’s high-sensitivity 16-bit digitization mode with a rolling (electronic) shutter. In this mode, one detected photon results in two “counts” on the camera. Our count rate data, measured in counts per pixel per measurement time, is roughly analogous to average current measurements in an ionization chamber.

2.1. System stability

Typical data from the experiment is shown in Fig. 2(a). For this data we place a $10\mu\text{Ci}$ Cs-137 D-disk source in direct contact with the NaI crystal housing so that the system approximates a 2π detector. The NaI crystal is placed as close as conveniently possible to the camera without any other optical elements. The camera integration time is set to 60 seconds. For

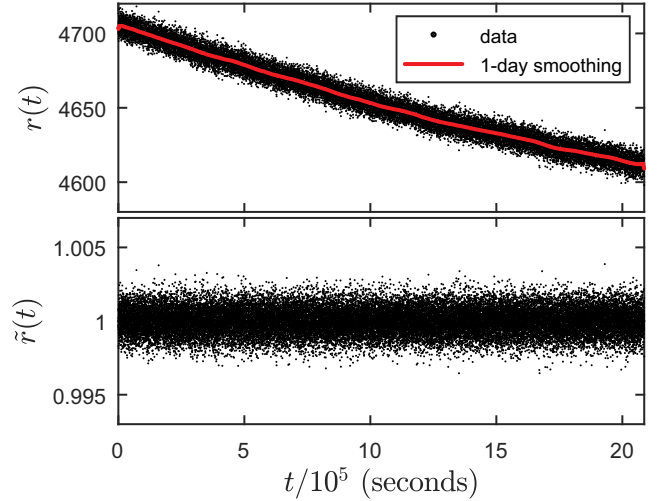


Figure 2: (color online) Data used for stability analysis of the CMOS camera using a $10\mu\text{Ci}$ Cs-137 gamma source. (a) The measured average number of counts per pixel per measurement time, $r(t)$, plotted as black dots. Each dot is the average signal over a 60 second interval. We observe a decline of roughly 2%, apparently due to a stability, dark signal, or amplifier gain drift in the camera. Also shown is a line that represents the data smoothed on a one day time scale. (b) The detrended count rate, $\tilde{r}(t)$, as defined in the text.

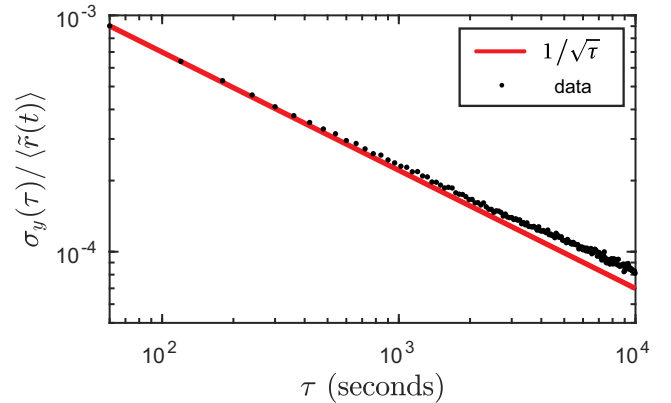


Figure 3: (color online) The standard deviation of the detrended data in Fig. 2(b) as a function of the averaging time τ .

this test, we do not correct for the dark signal, and we do not subtract off the small signal bias associated with the readout process (fixed-pattern read noise). This is a direct test of the uncorrected stability of the scintillator-plus-camera. Over the measurement time, the Cs-137 activity is essentially constant. The camera pixels are binned into 8×8 “super-pixels,” and the average number of photo-electrons per super-pixel, $r(t)$, is close to 5000 in 60 seconds.

In Fig. 2(a), the measured count rate $r(t)$ drifts downward by a few percent in over a period of about 24 days. To understand the ultimate stability limit of the detection system, we separate variability into two different time-scales—short term “noise” and long-term “drift.” To remove the long-term drift, we compare the individual data points to the average of the surrounding day’s data. This daily smoothing is shown as the solid line in Fig. 2(a). The corrected signal $\tilde{r}(t)$, defined as the ratio

of the raw data to the daily smoothing, is plotted in Fig. 2(b).

With the long-term drift removed, we analyze the remaining short-term noise in Fig. 2(b) by averaging the corrected data $\tilde{r}(t)$ over successively longer time intervals, and calculating the standard deviation of these averages. The standard deviation of $\tilde{r}(t)$ as a function of the averaging time τ is plotted in Fig. 3. This shows that the statistical errors reach below 0.01% in about 2 hours of data for the 10 μ Ci sample. In principle, this level of uncertainty could be reached faster by measuring a sample with higher activity.

Understanding the long-term drift in Fig. 2(a) is critically important. It is not clear if this drift arises from the NaI crystal or from the camera electronics. We have seen both positive and negative drifts of similar fractional size while measuring NaI scintillation from long-lived radio-isotopes and also while measuring a strongly attenuated intensity-stabilized laser. This might suggest that the problem lies in the camera. However, given our observations in Sec. 2.3, we cannot conclusively eliminate NaI as a possible source of signal drift.

As we have shown in a previous publication, ratio measurement techniques can remove detector drifts [2]. If we consider alternating measurements of two samples over a 4-hour time period, a drift of 2% in a week divides out to 0.04% in four hours. For measurements intended to detect drifts smaller than this, the source of the instability plotted in Fig. 2 will need to be reduced.

2.2. System linearity

We characterize the linearity of the detection system by measuring the decay of short-lived radio-isotopes over several half-lives. Measurements in Tc-99m, with a half-life of $\tau_{1/2} = 6.0067 \pm 0.0010$ days, and F-18, with a half-life of $\tau_{1/2} = 1.82890 \pm 0.00023$ days [1], are shown in Fig. 4. These samples contain the radio-isotopes in a liquid form as a pertechnetate for Tc-99m or fludeoxyglucose for F-18. These samples are held in a sealed plastic syringe above the NaI crystal. The crystal subtends a solid angle of 1.0 sr. In this configuration, a 10 mCi sample exposes the crystal to 3×10^7 gamma's per second (30 MBq).

The Tc-99m and F-18 scintillation data is recorded using the camera's 16-bit image mode. In this mode, the camera uses a dual-amplifier configuration in order to achieve the maximum dynamic range. One amplifier is optimized for large signals, and the other is optimized for low signals. These amplifiers are not perfectly matched, causing the signal to be slightly "s"-shaped relative to the expected exponential decay. In addition, there may be nonlinearities in the NaI crystal scintillation. However, we use the measured Tc-99m itself to linearize the overall system response. We find that this linearization can be successfully applied to measurements of other isotopes. This linearization gives excellent results for measurements spanning more than three orders of magnitude in activity level.

In Fig. 4(a), we show the measured decay signal (black dots) and the expected decay signal (red line) for a 3 mCi Tc-99m source. We correct for the amplifier response using the ratio of the measured signal vs. time for this source to the known

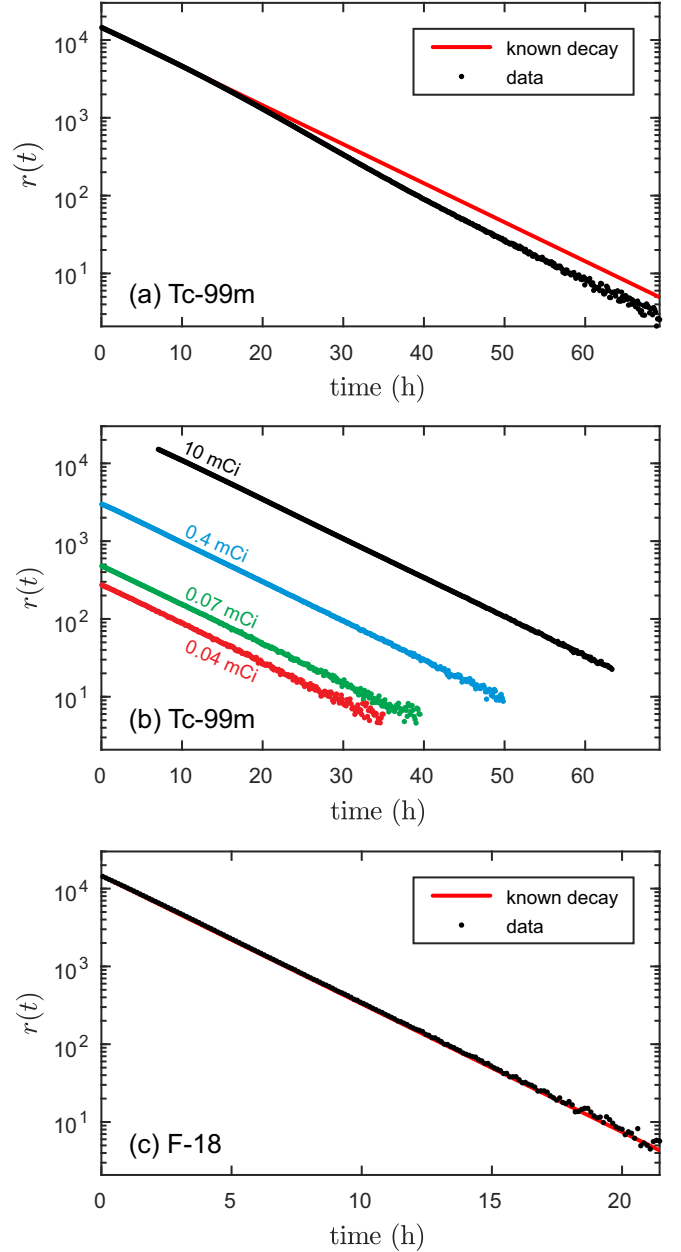


Figure 4: (color online) Linearity measurements and correction using short-lived radio-isotopes. (a) Tc-99m. The black dots are the measured count rates and the red line shows the expected count rate using the known half-life. The departure from exponential decay is due to amplifier nonlinearity in the camera. The initial sample activity is approximately 3 mCi. (b) Tc-99m data. The black dots are the same data from panel (a), with the linearization correction applied. The other data show the linearized measurements of lower activity samples. The four fitted half-lives for this data are average to 6.00(2) days, close to the accepted value of 6.0067(10) days. (c) F-18 data. The raw data is linearized using the Tc-99m correction. This produces a F-18 half life that is within 1% of the accepted value. The black dots are the linearized data, the red line is a fit with the known decay half-life. The initial F-18 sample activity is about 3 mCi.

decay rate. In Fig 4(b) we apply this correction to four subsequent measurements of Tc-99m samples with different activities (10 mCi, 0.4 mCi, 0.07 mCi, and 0.04 mCi). The linearization is excellent, reproducing the known half-life with sub-percent residuals. We also measure the decay of a 3 mCi F-18 source and apply the same linearity correction we used for the Tc-99m sample. The result is shown in Fig. 4(c). The fitted lifetime matches the known lifetime with an error of less than 1%. As an additional check of the system linearity, we measure the signal from several I-125 seeds. This isotope is a low-energy gamma emitter with a half life of 59.388(28) days [1]. We place different activity samples in front of the NaI crystal and measure the system response. The ratio of the measured response to the known source activity matches the linearity function obtained from the Tc-99m measurements to within the experimental uncertainties.

2.3. Hour-long time-response of NaI

Finally, we turn to the time-dependence of the NaI scintillation when measuring high activity samples. It is important to note that our detection system is immune to pulse pile-up systematics. This is demonstrated in Fig. 4, where samples ranging from 0.04 to 10 mCi can be measured without using any dead time correction.

Data in Fig. 5 show measurement data $r(t)$ of the first two hours of three different Tc-99m samples, normalized by the initial signal $r(0)$ measured just after the sample is placed on the detector. This data is taken from the same data sets used in Fig. 4. However, for that plot, the first few hours of nonlinear behavior was not used.

Figure 5 shows a nonlinear response of the NaI scintillation which increases with increasing activity levels. For samples with higher activity rates, the NaI crystal takes longer to reach its steady state. For the samples used in this study, this can take as long as a few hours. However, when steady state is reached, the analysis in Fig. 4 suggests that the decay of the short-lived Tc-99m and F-18 isotopes can be accurately measured. There is some indication in our data that NaI also takes some time to become completely dark after a high-activity sample is removed from proximity to the crystal.

This short-term instability for NaI is inconvenient. It might be possible to overcome the long-term stability issues using ratio measurements [2]. This would require excellent statistics for measuring high activity samples on the hour-long time scale. Unfortunately, this is precisely the time scale for short-term drifts in NaI response.

3. Conclusion

We report characteristics of a gamma-radiation detector based on a NaI crystal and a scientific camera. The system is capable of measuring high activity levels without dead time correction. With proper linearization, this detector accurately measures short-lived radioisotopes over three decades of dynamic range. We observe short-term changes in the NaI scintillation level at high activity. We also observe long-term instabilities

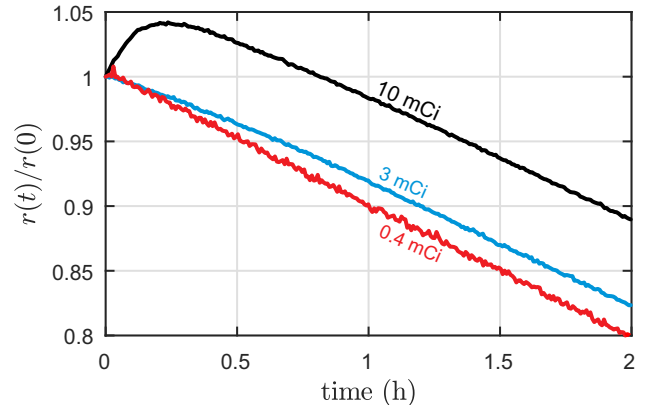


Figure 5: (color online) Measurements of three different Tc-99m samples for the first two hours. The three measurements have been normalized so that the data overlap at time zero, when the sample is first placed on the detector. The 0.3 mCi source closely approximates the expected Tc-99m decay. The time-dependent intensity non-linearity increases with sample activity, and more time is required before the data approaches the expected exponential decay. Using laboratory light sources, we verify that this behavior is not due to the camera, but rather arises from the NaI crystal itself. Note that the early time data leading to this effect was not included in the linearity measurements of Fig. 4.

of a few percent that may be attributable to the camera, the NaI crystal, or both. These drift characteristics must be considered for high precision measurements of seasonal fluctuations in the nuclear decay rates.

Future work will need to isolate the source of drift seen in Fig. 2. The camera could be tested in a better temperature-controlled environment using an intensity-controlled light source of verified stability. Future work should also study the response linearity of other suitable scintillation materials. The analysis in Fig. 3 suggests that it should be possible to reach a fractional accuracy of 0.0001% in 7 days for a 1 mCi sample, assuming that all sources of drift have been corrected. The camera+scintillator system is capable of measuring even higher activity sources. However, it will require a more linear scintillator than NaI.

References

- [1] Laboratoire Henri Becquerel, Recommended Values. http://www.nucleide.org/DDEP_WG/DDEPdata.htm, 2016. Accessed: 2016-09-23.
- [2] S. Bergeson, J. Peatross, and M. Ware. Precision long-term measurements of beta-decay-rate ratios in a controlled environment. *Physics Letters B*, 767:171 – 176, 2017.
- [3] S. Caccia, G. Bertuccio, D. Maiocchi, et al. A mixed-signal spectroscopic-grade and high-functionality cmos readout cell for semiconductor x-γ ray pixel detectors. *IEEE Transactions on Nuclear Science*, 55(5):2721–2726, Oct 2008.
- [4] J. H. Jenkins, E. Fischbach, J. B. Buncher, et al. Evidence of correlations between nuclear decay rates and Earth–Sun distance. *Astroparticle Physics*, 32(1):42 – 46, 2009.
- [5] F. Lebrun, J. P. Leray, P. Lavocat, et al. ISGRI: The INTEGRAL Soft Gamma-Ray Imager. *Astron. Astrophys.*, 411:L141–L148, Nov. 2003.
- [6] D. Meier, A. Czermak, P. Jalocha, et al. Silicon detector for a comp-ton camera in nuclear medical imaging. In *2000 IEEE Nuclear Science Symposium. Conference Record (Cat. No.00CH37149)*, volume 3, pages 22/6–2210 vol.3, 2000.

- [7] C. M. Michail, V. A. Spyropoulou, G. P. Fountos, et al. Experimental and theoretical evaluation of a high resolution cmos based detector under x-ray imaging conditions. *IEEE Transactions on Nuclear Science*, 58(1):314–322, Feb 2011.
- [8] B. W. Miller, L. R. Furenlid, S. K. Moore, et al. System integration of fastspect iii, a dedicated spect rodent-brain imager based on bazookaspect detector technology. In *2009 IEEE Nuclear Science Symposium Conference Record (NSS/MIC)*, pages 4004–4008, Oct 2009.
- [9] B. W. Miller, S. J. Gregory, E. S. Fuller, et al. The iqid camera: An ionizing-radiation quantum imaging detector. *Nuclear Instruments and Methods in Physics Research Section A: Accelerators, Spectrometers, Detectors and Associated Equipment*, 767:146 – 152, 2014.
- [10] O. Nähle and K. Kossert. Comment on “comparative study of beta-decay data for eight nuclides measured at the physikalisch-technische bundesanstalt” [astropart. phys. 59 (2014) 47–58]. *Astroparticle Physics*, 66:8 – 10, 2015.
- [11] M. Nikl. Scintillation detectors for x-rays. *Measurement Science and Technology*, 17, 2006.
- [12] T. E. Peterson and L. R. Furenlid. SPECT detectors: the anger camera and beyond. *Phys. Med. Biol.*, 56, 2011.
- [13] S. Pommé, H. Stroh, J. Paepen, et al. Evidence against solar influence on nuclear decay constants. *Physics Letters B*, 761:281 – 286, 2016.
- [14] H. Schrader. Seasonal variations of decay rate measurement data and their interpretation. *Applied Radiation and Isotopes*, 114:202 – 213, 2016.
- [15] C. Stapels, W. G. Lawrence, J. Christian, et al. Solid-state photomultiplier in cmos technology for gamma-ray detection and imaging applications. In *IEEE Nuclear Science Symposium Conference Record, 2005*, volume 5, pages 2775–2779, Oct 2005.
- [16] M. J. Ware, S. D. Bergeson, J. E. Ellsworth, et al. Instrument for precision long-term beta-decay rate measurements. *Review of Scientific Instruments*, 86(7), 2015.